EBioMedicine 43 (2019) 501–512

Contents lists available at ScienceDirect

EBioMedicine

journal homepage: www.ebiomedicine.com

EBioMedicine
Published by THE LANCET

Research paper

A PDGFRβ-based score predicts significant liver fibrosis in patients with chronic alcohol abuse, NAFLD and viral liver disease

Joeri Lambrecht [a], Stefaan Verhulst [a], Inge Mannaerts [a], Jan-Peter Sowa [c], Jan Best [c], Ali Canbay [c], Hendrik Reynaert [a,b], Leo A. van Grunsven [a,*]

[a] Department of Basic (Bio-)medical Sciences, Liver Cell Biology Research Group, Vrije Universiteit Brussel, Brussels, Belgium
[b] Department of Gastroenterology and Hepatology, University Hospital Brussels (UZBrussel), Brussels, Belgium
[c] Department of Gastroenterology, Hepatology and Infectious Diseases, University Hospital Magdeburg, Magdeburg, Germany

ARTICLE INFO

Article history:
Received 28 February 2019
Received in revised form 18 April 2019
Accepted 18 April 2019
Available online 27 April 2019

Keywords:
Platelet derived growth factor receptor
Biomarker
Extracellular vesicle
Diagnosis
Hepatic stellate cell

ABSTRACT

Background: Platelet Derived Growth Factor Receptor beta (PDGFRβ) has been associated to hepatic stellate cell activation and has been the target of multiple therapeutic studies. However, little is known concerning its use as a diagnostic agent.
Methods: Circulating PDGFRβ levels were analysed in a cohort of patients with liver fibrosis/cirrhosis due to chronic alcohol abuse, viral hepatitis, or non-alcoholic fatty liver disease (NAFLD). The diagnostic performance of PDGFRβ as individual blood parameter, or in combination with other metabolic factors was evaluated.
Findings: sPDGFRβ levels are progressively increased with increasing fibrosis stage and the largest difference was observed in patients with significant fibrosis, compared to no or mild fibrosis. The accuracy of sPDGFRβ-levels predicting fibrosis could be increased by combining it with albumin levels and platelet counts into a novel diagnostic algorithm, the PRTA-score, generating a predictive value superior to Fib-4, APRI, and AST/ALT. The sPDGFRβ levels and the PRTA-score are independent of liver disease aetiology, thus overcoming one of the major weaknesses of current non-invasive clinical and experimental scores. Finally, we confirmed the diagnostic value of sPDGFRβ levels and the PRTA-score in an independent patient cohort with NAFLD which was staged for fibrosis by liver biopsy.
Interpretation: The PRTA-score is an accurate tool for detecting significant liver fibrosis in a broad range of liver disease aetiologies.
Fund: Vrije Universiteit Brussel, the Institute for the Promotion of Innovation through Science and Technology in Flanders (IWT-Flanders) (HILIM-3D; SBO140045), and the Fund of Scientific Research Flanders (FWO).

1. Introduction

The chronic presence of liver-injury causing agents, including alcohol, Hepatitis B or C virus (HBV/HCV) infection, and non-alcoholic steatohepatitis/fatty liver disease (NASH/NAFLD), leads to the activation of hepatic stellate cells (HSCs) toward a myofibroblastic phenotype [1]. This activation process is characterized by an excessive deposition of extracellular matrix, scar tissue formation, and an enhanced responsiveness of the HSCs toward various stimulating factors secreted by their microenvironment [2]. Such enhanced responsiveness is facilitated by an elevated expression of cell membrane receptors such as several tyrosine kinases receptors [2]. One such receptor is the platelet derived growth factor receptor (PDGFR), of which 2 variants can be found: PDGFR-alpha (PDGFRα) which is constitutively expressed by HSCs, and PDGFR-beta (PDGFRβ) whose expression increases during HSC activation [3]. Binding of the PDGF isoforms to their respective receptors induces receptor dimerization, phosphorylation of tyrosine residues at

Abbreviations: PDGFRβ, platelet derived growth factor receptor beta; sPDGFRβ, soluble pdgfrβ; AUC, area under the curve; PRTA-score, Spdgfrβ thrombocyte albumin score; Fib-4, fibrosis-4; APRI, AST to platelet ratio index; AST, aspartate aminotransferase; ALT, alanine aminotransferase; HBV, Hepatitis B virus; HCV, Hepatitis C virus; NASH, non-alcoholic steatohepatitis; NAFLD, non-alcoholic fatty liver disease; HSC, hepatic stellate cell; PDGFRα, platelet derived growth factor receptor alpha; ARFI, acoustic radiation force impulse; MRE, magnetic resonance elastography; ELF, enhanced liver fibrosis; IU/L, International units per litre; ULN, upper limit of normal; NPF, non-parenchymal fraction; FACS, fluorescence-activated cell sorting; CCl_4, carbon tetrachloride; PBS, phosphate buffered saline; EV, extracellular vesicle; NTA, nanoparticle tracking analysis; GAPDH, glyceraldehyde 3-phosphate dehydrogenase; αSMA, alpha smooth muscle actin; HSP70, heat shock protein 70; ELISA, enzyme-linked immunosorbent assay; SD, standard deviation; ROC, receiver operating characteristics; BMI, body mass index; ECM, extracellular matrix; KC, Kupffer cell; LSEC, liver sinusoidal endothelial cell; RNA, ribonucleic acid; WB, Western blot; n, number; IQR, interquartile range; Alk phos, alkaline phosphatase; GGT, gamma-glutamyl transferase; CI, confidence interval; ALD, alcoholic liver disease.

* Corresponding author at: Vrije Universiteit Brussel, Faculty of Medicine and Pharmacy, Department of Basic (Bio-)medical Sciences, Liver Cell Biology Research Group, Laarbeeklaan 103, 1090 Brussels (Jette), Belgium.
E-mail address: lvgrunsv@vub.be (L.A. van Grunsven).

https://doi.org/10.1016/j.ebiom.2019.04.036

Research in context

Evidence before this study

Alcoholism, obesity, and virus infection all may lead to damage and stiffening of the liver, resulting in the loss or limitation of some vital liver functions. If untreated, this condition may even result in the development of liver cancer. Screening of patients that are at risk or are in early development of such liver fibrosis is thus highly needed. However, till date, the most sensitive manner to diagnosis early-stage liver fibrosis remains the liver biopsy, an invasive procedure which can cause discomfort for the patient and which demands significant financial input by the health care system. Multiple novel non-invasive scoring systems have been proposed but lack sufficient sensitivity and specificity to identify and distinguish between the early stages of liver fibrosis.

Added value of this study

In this study, we gathered a cohort of patients with liver fibrosis/cirrhosis due to chronic alcohol abuse, viral hepatitis, or non-alcoholic fatty liver disease (NAFLD). Blood-analysis identified an enhanced expression of the activated hepatic stellate cell (HSC)-marker PDGFRβ in patients with significant fibrosis, compared to those with no or mild fibrosis. We found that when we combined such PDGFRβ levels with albumin levels and thrombocyte counts into a novel diagnostic algorithm, the PRTA-score, the clinical used serological scores Fib-4, APRI, and AST/ALT were outperformed. In conclusion, this research proposes the novel diagnostic PRTA-algorithm, an easy applicable, low cost and accurate scoring for significant liver fibrosis in a broad range of liver disease aetiologies.

Implications of the available evidence

Our novel serological diagnostic tool will allow wide-scale screening of patients that are at risk, by a simple blood-analysis that can be performed by the general practitioner, identifying those patients that are suitable to start treatment. Additionally, use of our scoring system may reduce the number of needed liver biopsies, what will not only have a positive financial impact, but will also increase the willingness of patients to participate in follow up studies.

the intracellular domain of the receptor, and activation of various pro-fibrogenic cascades [2,4].

Diagnosis of liver fibrosis onset and progression remains an important issue in the current clinical settings. The gold standard, and the diagnostic tool with highest specificity and sensitivity, remains the liver biopsy, an invasive procedure associated with multiple drawbacks including inter-and intra-observer variability [5], discomfort for the patient such as pain and post-procedure complications [6], and a questionable cost-benefit ratio [7]. In order to overcome these drawbacks, multiple non-invasive diagnostic tools have been proposed [8]. Imaging modalities are a subgroup of such non-invasive diagnostic tools, measuring the elastic properties and stiffness of the liver tissue [9]. Transient elastography (such as FibroScan®) [10] and acoustic radiation force impulse (ARFI) [11] are examples which have been validated in various aetiologies of liver disease. Furthermore, the use of serological markers has been proposed for non-invasive assessment of liver fibrosis. The use of serum markers may rely on the detection of a single parameter, or a group of parameters combined into a diagnostic algorithm [8]. In the current clinical setting, several serological algorithms have gained popularity, such as the fibrosis 4 (Fib-4) score [12], enhanced liver fibrosis (ELF) test [13], aspartate aminotransferase/alanine aminotransferase (*AST/ALT*) *ratio* [14], and the AST to platelet ratio index (APRI) [15]. However, although the implementation of serological markers and imaging modalities has led to less liver biopsies, it has not yet resulted into its full redundancy. Avoidance of liver biopsy for staging of fibrosis will only be possible when a non-invasive marker has been found which is independent of liver disease aetiology, easily accessible, with low cost, and with high specificity and sensitivity for both early and late stages of liver fibrosis [16]. Especially the limited accuracy for diagnosis and progression of early stage liver fibrosis remains a weakness of current non-invasive diagnostic tools, which thus prevents an as early as possible therapeutic intervention (or life style change) to avoid fibrosis progression. As fibrosis has been shown to be the most important predictor of liver-related mortality [17], early intervention would significantly reduce mortality.

In this study, we present an analysis of circulating PDGFRβ protein levels in a patient population with different aetiologies of liver fibrosis, being chronic alcohol abuse, chronic viral (HBV/HCV) infection and NAFLD. Additionally, we propose the implementation of soluble PDGFRβ levels into a novel diagnostic algorithm, the sPDGFRβ thrombocyte albumin (PRTA)-score, which yields a high discriminative capacity for diagnosis of significant fibrosis.

2. Materials and methods

2.1. Animal studies

The use and care of animals was reviewed and approved by the Ethical Committee of Animal Experimentation of the Vrije Universiteit Brussel (VUB, Belgium) in project 16-212-2, and was carried out in accordance to European Guidelines for the Care and Use of Laboratory Animals. Mice were housed in a controlled environment with free access to chow and water. Quiescent hepatic stellate cells were isolated from male Balb/c mice (Charles River Laboratories, L'Arbresle, France) (25–30 weeks old) as described earlier [18]. Briefly, murine livers were perfused with enzymatic solutions, followed by low-speed centrifugation steps to remove hepatocytes. Hepatic stellate cells were purified from the non-parenchymal fraction based on their buoyancy, using an 8% Nycodenz solution. Isolated HSCs were cultured on regular tissue culture dishes (Greiner Bio-One, Vilvoorde, Belgium), in Dulbecco's modified Eagle's medium (Lonza, Verviers, Belgium) supplemented with 10% exosome-depleted foetal bovine serum (System Biosciences, Mountain View, USA), 2 Mm L-glutamine (Ultraglutamine 1®) (Lonza), 100 U/ml penicillin and 100 μg/ml streptomycin (Pen-Strep®) (Lonza), inducing an in vitro myofibroblastic transdifferentiation.

The different liver cell populations were isolated based on cell-type specific protein expression, as described earlier [19]. Briefly, murine livers were perfused with enzymatic solutions, followed by low-speed centrifugation steps to separate the non-parenchymal fraction from the hepatocyte population. The non-parenchymal fraction (NPF) was incubated with anti-F4/80-APC (MF8021, Thermo Scientific, USA) and anti-CD32-PE (ab30357, Abcam, UK). NPF was then analysed with FACS (FACS Aria II, Becton-Dickinson, Belgium) and used to isolate liver sinusoidal endothelial cells (LSEC, CD32 + F4/80-UV-), Kupffer cells (CD32-F4/80 + UV-) and HSCs (CD32-F4/80-UV+).

For in vivo induction of liver fibrosis, 10-week old mice received 8 intraperitoneal injections of 15 μl carbon tetrachloride (CCl_4) diluted in 85 μl mineral oil (Sigma-Aldrich, St. Louis, MO, USA) per 30 g bodyweight over a period of 4 weeks. Mice were sacrificed 24 h after the last injection.

2.2. Cell-derived extracellular vesicle (EV) isolation

Conditioned medium was collected from cultured mouse HSCs after 2 days or 10 days of culture (new medium was added every 2 days) and

cleared from cellular debris by centrifugation at 300 *g* for 5 min (4 °C) and 2500 g for 20 min (4 °C). Large vesicle-like contaminants were depleted by centrifugation at 10,000*g* for 30 min. The supernatant was further centrifuged at 100,000*g* for 2 h (4 °C) to pellet EVs, which were then washed once by resuspension in phosphate-buffered saline (PBS) followed by a final ultracentrifugation step at 100,000*g* for 2 h (4 °C). The final EV pellet was resuspended in a small volume of PBS and characterized by use of the ZetaView® PMX110 (Particle Metrix, Meerbusch, Germany) which is equipped with nanoparticle tracking analysis (NTA) software, for particle size, zeta-potential, and concentration. The instrument was calibrated using 100 nm sized polystyrene particles and handled following manufacturer's protocol. NTA measurements were executed at 11 different positions at a constant temperature of 23 °C.

2.3. Initial patient cohort

Patients were recruited from the Department of Gastroenterology of the University Hospital of Brussels (UZ Brussel), Belgium. The study protocol was approved by the local ethical committee of the UZ Brussel and Vrije Universiteit Brussel (reference number 2015/297; B.U.N. 143201525482) and was in accordance with the Declaration of Helsinki. Patients with alcohol abuse, chronic viral hepatitis and NAFLD were recruited. A healthy population that had no evidence of liver disease was recruited as control group. All participants signed an informed consent prior to inclusion to the study. Inclusion criteria for fibrosis and cirrhosis patients included: i) diagnosis confirmed by elastography; ii) availability of complete clinical information. Exclusion criteria were: i) HIV co-infection; ii) missing data on important variables; iii) idiopathic/unknown origin of liver disease. Diagnosis of liver fibrosis and cirrhosis was based on physical examination, blood tests, and elastography techniques. Patients with viral or alcoholic liver disease underwent transient elastography (FibroScan®, Echosens, France). Patients with at least 10 valid liver stiffness measurements with a success rate of at least 60% were included in the final analysis. Cut-off values used to discriminate fibrotic stages equal or more than F2, F3 or F4, were respectively 7.2 kPa, 9.5 kPa and 12.5 kPa [20]. Acoustic radiation force impulse (ARFI) was applied to determine the stage of liver fibrosis in those patients with NAFLD. Cut-off values of 1.25 m/s, 1.54 m/s and 1.84 m/s were used to identify a fibrotic stage equal to, or more than F2, F3, and F4 respectively.

2.4. Blood collection

Blood samples were collected by venepuncture into evacuated EDTA-KE S-Monovette tubes (Sarstedt AG & Co, Nümbrecht, Germany) on the day of liver biopsy or elastography. Blood specimens were subjected to haematological and biochemical analyses. Plasma was created within maximum 2 h after collection, using a two-step centrifugation protocol consisting of 1500*g* for 10 min (4 °C) and 2000*g* for 3 min (4 °C). Plasma was frozen at −80 °C until use.

2.5. Serological tests

Validation of the suggested fibrosis scoring was obtained by haematological analysis and diagnostic algorithms such as the NAFLD fibrosis score, Fib-4, APRI, and AST/ALT ratio. Fib-4 and APRI were calculated using following formulae:

$$\text{FIB 4} = \text{age} \times \text{AST [IU/L]} / \left(\text{platelet count}\left[10^9/\text{L}\right] \times (\text{ALT [IU/L]})^{1/2}\right)$$

$$\text{APRI} = (\text{AST[IU/L]/ULN}) / \text{platelet count}\left[10^9/\text{L}\right]$$

2.6. Human liver tissue

Human liver tissue (Supplementary Table 1) was obtained from surgical procedures performed at the Department of Thoracic and Transplantation Surgery and Surgical Oncology of the University Hospital of Brussels (UZ Brussel), Belgium. Ethical approval was obtained from the local ethical committee of the UZ Brussel (Reference number 2015/278; B.U.N. 143201525406) and was in accordance with the Declaration of Helsinki. All participants signed an informed consent prior to inclusion to the study.

2.7. Validation patient cohort

For validation, 57 NAFLD-patients were recruited from a cohort initially recruited at the Alfried-Krupp-Krankenhaus Essen, Department for General and Visceral Surgery, Germany. The study protocol was approved by the institutional review board of the University Hospital Essen (Ethik-Kommission der Medizinischen Fakultät der Universität Duisburg-Essen; Germany; reference number 15-6356-BO) and was in accordance with the Declaration of Helsinki. All procedures adhered to the Declaration of Helsinki and the requirements of the IRB. Due to the retrospective nature of the validation study the IRB waived the need for written informed consent.

Patients of this cohort received bariatric surgery for weight reduction due to morbid obesity. Patients were eligible for the validation study, when liver histology, including fibrosis scoring, and a sufficient amount of serum was available. Patients received dietary and exercise counselling for 6 months prior surgery, without calorie restriction. A blood sample was collected for assessment of serum derived factors on the day of surgery (prior surgery) and liver tissue was sampled during bariatric surgery as a wedge biopsy. All data shown were recorded on the day of surgery.

Histological assessment of the liver tissue (steatosis, ballooning, lobular inflammation and fibrosis) was performed by two expert pathologists on HE- and Masson's Trichrome stained 4 μm slides for each sample according to Kleiner et al. [21] and Desmet et al. [22].

2.8. Human hepatic stellate cells

Primary human HSCs were purchased from ScienCell (San Diego, USA), and used before passage 8 was reached. The LX-2 cell line, an immortalized human HSC line, was kindly provided by Dr. Scott L. Friedman (Mount Sinai School of Medicine, New York, USA). Human HSCs were cultured in Dulbecco's modified Eagle's medium (Lonza) supplemented with 10% exosome-depleted foetal bovine serum (System Biosciences), 2 Mm L-glutamine (Ultraglutamine 1®) (Lonza), 100 U/ml penicillin and 100 μg/ml streptomycin (Pen-Strep®) (Lonza).

2.9. Enzyme-linked immunosorbent assays (ELISA)

Human soluble PDGFRβ was measured with a commercially available ELISA kit (ThermoFisher scientific), according to manufacturer's instructions. All plasma samples were diluted 1/10 with diluent provided by the manufacturer. Absorbance values were obtained with an iMark™ microplate absorbance reader (Bio-rad).

2.10. Statistical analysis

Data was analysed using GraphPad Prism 6 (GraphPad, Palo Alto, USA) statistical software. Quantitative variables are expressed as means ± standard deviation (SD) or expressed as box-plots (min to max). Statistical analyses were performed using the Student's *t*-test, Mann-Whitney test, and Kruskal-Wallis test with Dunn's post hoc test, as appropriate. Categorical variables were analysed using the Chi-square test. The baseline characteristics of the three patient cohorts were compared using the Chi-square test or Kruskal-Wallis test. To

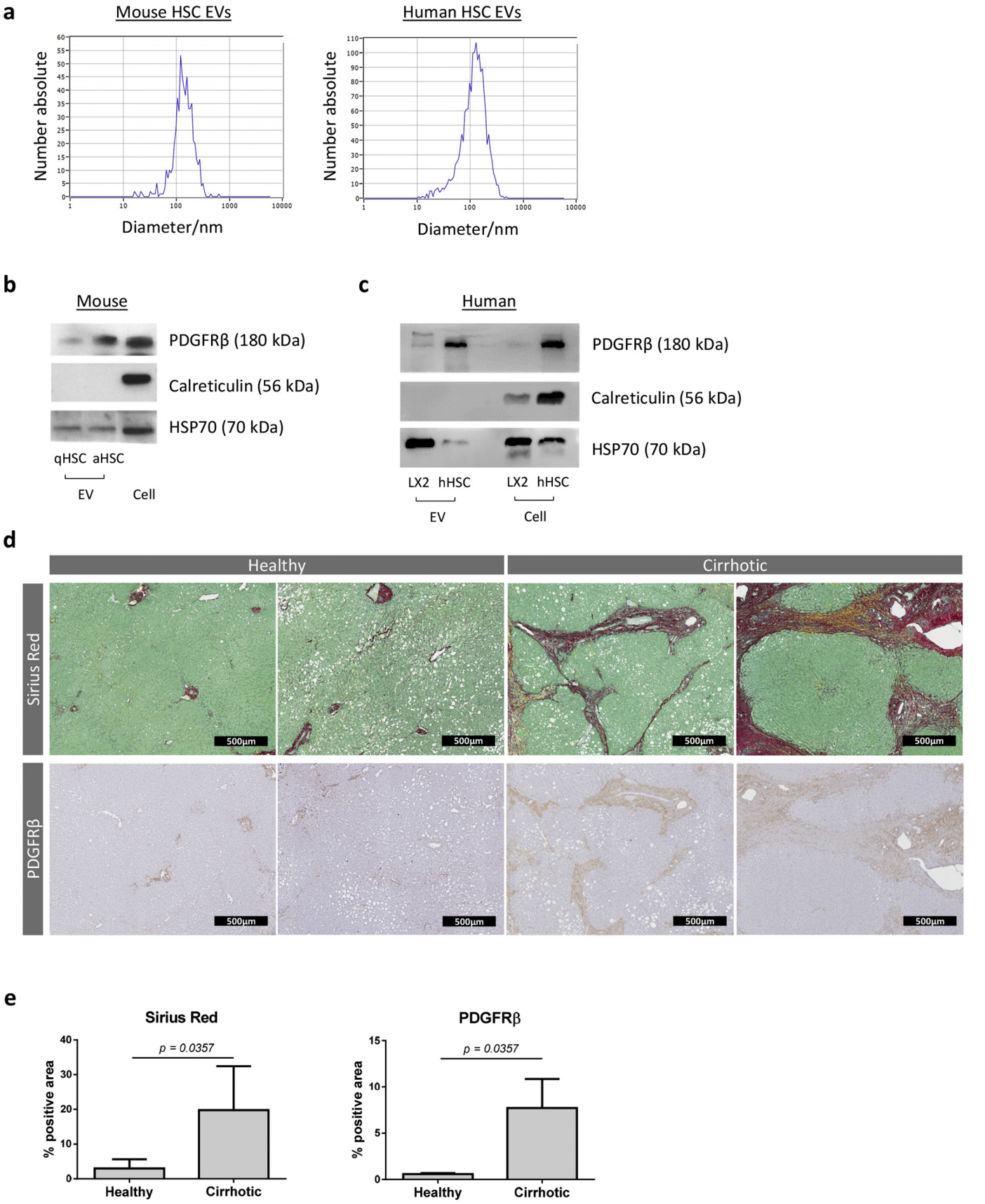
a
Mouse HSC EVs
Human HSC EVs
Number absolute
Diameter/nm
b
Mouse
PDGFRβ (180 kDa)
Calreticulin (56 kDa)
HSP70 (70 kDa)
qHSC aHSC
EV
Cell
c
Human
PDGFRβ (180 kDa)
Calreticulin (56 kDa)
HSP70 (70 kDa)
LX2 hHSC
LX2 hHSC
EV
Cell
d
Healthy
Cirrhotic
Sirius Red
PDGFRβ
500µm
e
Sirius Red
PDGFRβ
p = 0.0357
p = 0.0357
% positive area
Healthy
Cirrhotic

determine the diagnostic accuracy and performance, receiver operating characteristic (ROC) curves were constructed, and the area under the curve (AUC) was calculated. In order to identify ideal cut-off values, the Youden's index was calculated [23], and the sensitivity and specificity were computed. Correlation studies were executed using the Spearman's correlation test. The sufficiency of the sample size was confirmed by MedCalc version 18 (MedCalc Software, Ostend, Belgium) using in house preliminary results and a type I error rate (α) of 5% and a power (1-β) of 80%. Differences of obtained results were considered significant at $p < 0.05$.

3. Results

3.1. Human and murine aHSC-derived EVs are positive for PDGFRβ

We previously reported on the enhanced expression of PDGFRβ on extracellular vesicles (EVs) extracted from the plasma of chronic Hepatitis B or C virus (HBV/HCV)-infected patients with early (F ≤ 2) liver fibrosis [18]. This led us to speculate that these circulating EVs could represent the presence of activated HSCs in the injured liver. To investigate this hypothesis, we first verified the possible HSC-derived origin of these PDGFRβ-positive EVs. Vesicles extracted by ultracentrifugation from the culture medium of primary mouse- and human HSCs show an average size of 130 nm (Fig. 1a), which corresponds to the characteristic size of small vesicles [24]. Protein analysis further characterized these EVs through their positivity for the EV-marker Heat Shock Protein 70 (HSP70) and absence of the cellular marker calreticulin (Fig. 1b and c), indicative of pure EVs. Comparison of EVs extracted from media collected from activated primary mouse HSC cultures (culture day 8–10) to more quiescent HSC cultures (day 0–2), shows an enrichment in PDGFRβ (Fig. 1b). In line, a strong PDGFRβ-positivity can be seen in EVs derived from activated primary human HSCs (Fig. 1c). In contrast, the HSC cell line LX2 does not show an enrichment of PDGFRβ in their EVs (Fig. 1c).

To evaluate whether in human livers PDGFRβ expression is also correlated with the activated phenotype of HSCs, we evaluated liver tissue obtained from cirrhotic HCC patients. Picrosirius staining shows the excessive collagen deposition, and thus the fibrotic/cirrhotic character of liver tissue obtained from these HCC patients. Collagen deposition was absent or limited in healthy liver tissue obtained from patients undergoing resection of colorectal metastases (Fig. 1d, e). Together with the significant deposition of collagens in the fibrotic/cirrhotic tissue, we show a significant higher expression of PDGFRβ (Fig. 1d, e), confirming previous reports [25,26].

3.2. PDGFRβ is up-regulated in the murine CCl_4-injury model

We next analysed the expression of PDGFRβ in a well-established murine model of liver fibrosis, being repeated injections of carbon tetrachloride (CCl_4), in which chronic necro-inflammatory damage leads to a significant activation of HSCs [27]. Protein analysis of the livers of 4-week CCl_4-treated mice shows a significant up-regulation of PDGFRβ, both by western blot (Fig. 2a) and on staining (Fig. 2b), as compared to their healthy controls. RNA expression analysis shows a dominant expression of PDGFRβ in HSCs when compared to the non-parenchymal fraction (NPF), and to freshly isolated individual liver cell types being hepatocytes, liver sinusoidal endothelial cells, and Kupffer cells (Fig. 2c). This HSC-association of PDGFRβ is further illustrated by the correlation and overlap (Spearman's correlation coefficient (r) = 0.7838) in protein expression of PDGFRβ and alpha smooth muscle actin (αSMA), a marker for activated HSCs, in livers of CCl_4-treated mice (Fig. 2d).

3.3. Clinical characteristics of the initial study population

Due to the several drawbacks of vesicle research such as the time-consuming and low-throughput character of current EV isolation techniques, the clinical setting is currently not ready to use EVs, nor their protein content, as biomarkers for the diagnosis of disease onset or its progression [8]. We therefore investigated the possibility to use total circulating PDGFRβ content as biomarker for liver fibrosis progression. To this end, the plasma PDGFRβ-content of a cohort of 148 patients and 14 healthy volunteers was analysed. Patients with various aetiologies of liver disease were included, being chronic alcohol abuse ($n = 35$), chronic HBV/HCV infection ($n = 46$), and NAFLD ($n = 67$) (Table 1). As expected, a significantly higher Body Mass Index (BMI) value is observed in patients with NAFLD.

Patients with alcoholic or viral liver disease underwent transient elastography measurements by FibroScan® to determine the stage of fibrosis/cirrhosis. Patients with NAFLD all suffered from Diabetes Mellitus type 2 and underwent ARFI to evaluate the degree of liver fibrosis/cirrhosis. In the total patient cohort, stage of liver fibrosis was distributed as follows: F0–1, $n = 51$ (34.46%); F2, $n = 29$ (19.59%); F3, $n = 28$ (18.92%); and F4, $n = 40$ (27.03%). Various fibrosis scoring algorithms, including the aspartate aminotransferase/alanine aminotransferase (*AST/ALT*) *ratio*, AST to platelet ratio index (APRI), and Fibrosis-4 (Fib-4) index, were calculated to further validate the early or late disease-character of the included patients (Supplementary Table 2).

3.4. sPDGFRβ predicts the presence of significant (F ≥ 2) fibrosis

Analysis of soluble PDGFRβ (sPDGFRβ) levels in our total patient cohort by ELISA identified an overall increase of sPDGFRβ according to the stage of liver fibrosis (Fig. 3a). Creating various sub-populations based on staging of fibrosis identified a significant discriminative value of sPDGFRβ levels to distinguish patients with significant fibrosis (F ≥ 2) from those with no or minimal fibrosis (F0-1); (median [25th; 75th percentile]) 9317 [6625;12,333] pg/mL vs 5581 [3838;10,069] pg/mL, respectively, $p < 0.0001$. Use of sPDGFRβ to predict the presence of significant fibrosis (F ≥ 2) was assessed by construction of AUROC, and generated an AUC of 0.7303 (95% confidence interval (CI): 0.6395–0.8211) (Table 2), which is considerably higher than the AUCs obtained from clinical scores such as Fib-4, APRI and AST/ALT, respectively 0.6635 (95% CI: 0.5690–0.7581), 0.6309 (95% CI: 0.5331–0.7286), and 0.5976 (95% CI, 0.4952–0.7001) (Table 2).

When the cut-off for parting of the patient population is taken at advanced fibrosis (F ≥ 3) or cirrhosis (F = 4), significant differences with lower fibrosis stages can still be seen, respectively $p = 0.0079$ and $p = 0.0273$ (Fig. 3a). However, the predictive character of sPDGFRβ strongly decreases (F ≥ 3: 0.6446 (95% CI: 0.5565–0.7327); F = 4: 0.6409 (95% CI: 0.5457–0.7360)) (Table 2) and is lower than the calculated established clinical scores (Table 2).

3.5. Predictive function of sPDGFRβ is independent of disease aetiology

Division of the patient cohort based on disease aetiology identified the strongest discriminative function of sPDGFRβ for significant liver fibrosis (F ≥ 2) in patients with alcoholic liver disease; 0.8634 (95% CI:

Fig. 1. PDGFRβ-expression in HSC-derived EVs and human liver tissue. (a) Nanoparticle tracking analysis of purified EVs from murine and human HSCs. (b) Comparison of EVs derived from activated (aHSC, day 8 to 10 of culture) and quiescent mouse HSCs (qHSC, day 0–2 of culture) by WB analysis, using cell lysates of activated HSCs as control (whole western blot membrane for PDGFRβ is shown in Supplementary Fig. 1). EV-purity was verified by presence of the EV-marker HSP70 and absence of the cellular marker calreticulin. (c) WB analysis of EVs secreted by LX2s and activated primary human HSCs (hHSC), using their respective cell lysates as control (whole western blot membrane for PDGFRβ is shown in Supplementary Fig. 1). (d) Total liver tissue of healthy and cirrhotic patients analysed for collagen deposition (Sirius Red) and expression of PDGFRβ. Representative images are shown ($n \geq 3$). Black bars represent 500 μm. (e) The area of PDGFRβ-positive or Sirius Red-positive staining in healthy ($n = 5$) and cirrhotic ($n = 3$) patients was calculated by using image analysis software and is plotted as percentage of the total area. Error bars represent mean values ± SD.

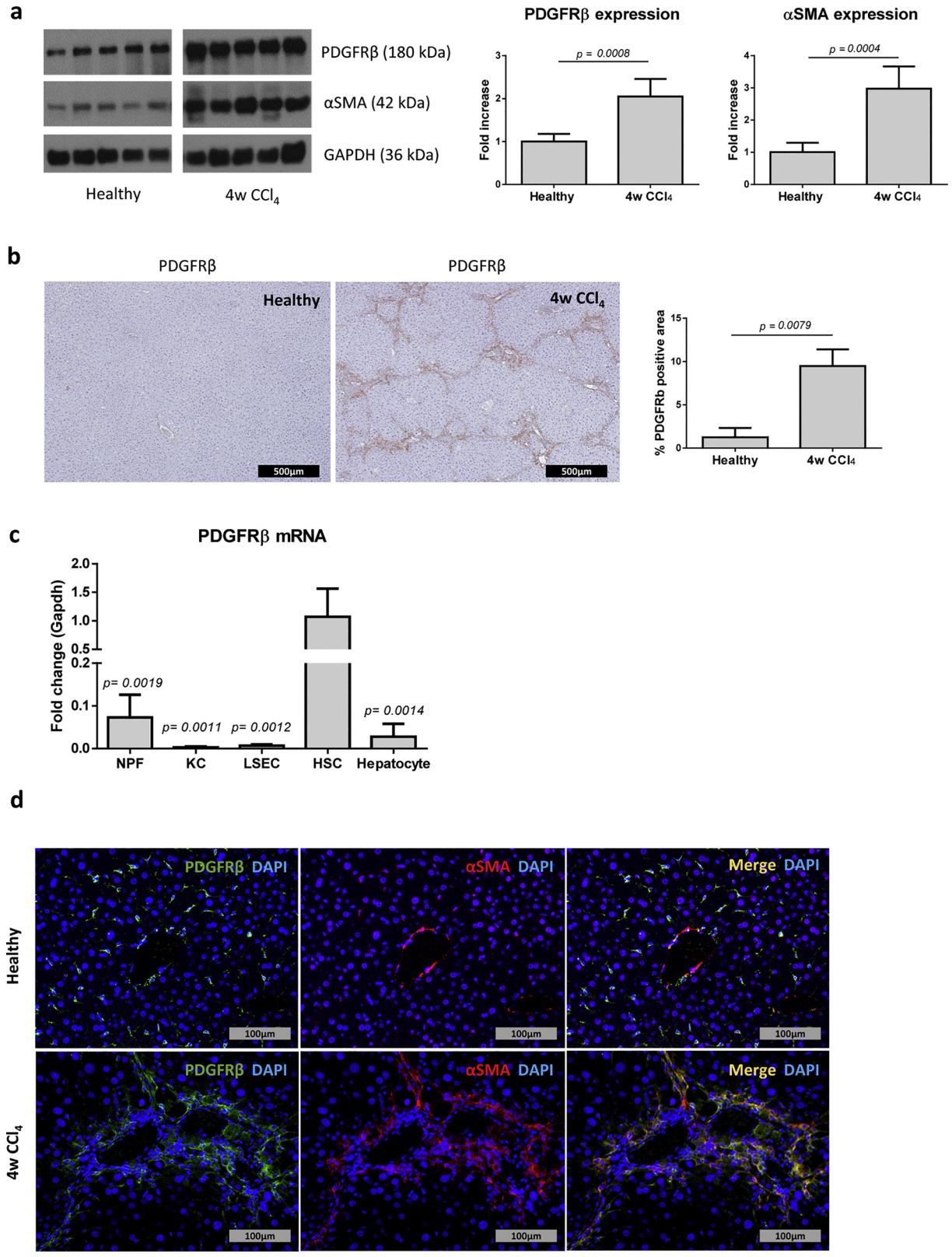

Fig. 2. PDGFRβ expression in a CCl_4-induced mouse model of liver fibrosis. PDGFRβ-expression in total liver tissue of CCl_4-injected mice, both on (a) WB and (b) immune histochemical staining. (a) PDGFRβ and αSMA protein levels were quantified and normalized versus GAPDH expression (n = 5) (whole western blot membrane for PDGFRβ is shown in Supplementary Fig. 1). Bars indicate the fold increase in CCl_4-treated mice compared to healthy controls. (b) Representative images of PDGFRβ-staining on liver tissue of healthy and CCl_4-induced mice are shown. Black bars represent 500 μm. The area of PDGFRβ positive staining was calculated by using image analysis software and is plotted as percentage of the total area (n = 5). (c) PDGFRβ mRNA expression in the non-parenchymal fraction (NPF) and different liver cell types, being quiescent HSCs, Kupffer cells (KC), liver sinusoidal endothelial cells (LSEC), and hepatocytes. Significant differences were calculated as compared to PDGFRβ mRNA expression in HSCs. Error bars represent mean values ± SD. (d) PDGFRβ expression by activated HSCs shown by co-staining of PDGFRβ and the activation marker αSMA in liver tissue of healthy or CCl_4-injured mice. Representative images are shown (n = 3). Grey bars represent 100 μm.

Table 1
Patient characteristics – cohorts based on aetiology of liver disease.

Liver disease aetiology	Alcoholic	Viral	NAFLD	*p*-value
Individuals, n	35	46	67	
Characteristics				
Age (years): median (IQR)	60 (53–63)	53 (41–64)	55 (52–64)	0.1008
Male, n (%)	26 (74.29%)	27 (58.69%)	42 (62.69%)	0.3292
BMI (kg/m^2): median (IQR)	26.23 (23.11–30.57)	24.30 (22.36–28.12)	32.68 (28.00–35.06)	<0.0001
Laboratory parameters: median (IQR)				
AST (IU/L)	57 (29–89)	40 (27–66)	40 (24–54)	0.0512
ALT (IU/L)	39 (26–61)	42 (30–74)	53 (38–77)	0.0182
Alk Phos (IU/L)	132 (89–174)	70 (57–86)	81 (62–108)	<0.0001
GGT (IU/L)	229 (81–951)	48 (19–138)	64 (39–139)	<0.0001
Total bilirubin (mg/dL)	1.17 (0.57–2.75)	0.67 (0.45–0.88)	0.66 (0.57–0.91)	0.0119
Albumin (g/L)	39 (31–42)	44 (41–46)	43 (40–44)	<0.0001
Thrombocytes (x10^3/mm^3)	165 (118–214)	205 (156–256)	231 (201–267)	0.0012
Creatinine (mg/dL)	0.81 (0.68–1.11)	0.84 (0.73–1.00)	0.81 (0.70–0.97)	0.7334
Fibrosis scoring: median (IQR)				
AST/ALT ratio	1.20 (0.89–2.23)	0.91 (0.79–1.17)	0.67 (0.61–0.81)	< 0.0001
APRI	0.74 (0.43–1.56)	0.50 (0.34–0.71)	0.30 (0.23–0.38)	<0.0001
Fib-4	2.86 (1.34–5.44)	1.90 (1.05–2.80)	1.28 (0.86–1.70)	<0.0001
NAFLD fibrosis score	/	/	−0.55 (−1.08–0.43)	
Fibroscan (kPa)	11.65 (6.03–51.78)	7.15 (4.60–11.78)	/	
ARFI (m/s)	/	/	1.32 (1.20–1.60)	

n: number; IQR: Interquartile range; BMI: Body Mass Index; AST: aspartate aminotransferase; ALT: alanine aminotransferase; Alk Phos: Alkaline phosphatase; GGT: gamma-glutamyl transferase; Fib-4: Fibrosis-4; AST/ALT-ratio: aspartate aminotransferase/alanine aminotransferase ratio; APRI: AST to platelet ratio index; ARFI: acoustic radiation force impulse; NAFLD: non-alcoholic fatty liver disease.

0.6836–1.043) (Supplementary Table 3). The AUC in patients with viral liver disease was 0.7253 (95% CI: 0.5732–0.8774) and in NAFLD 0.6406 (95% CI: 0.4825–0.7986). The predictive function of sPDGFRβ for significant liver fibrosis (F ≥ 2) is higher for all three disease aetiologies, separately, than the predictive accuracy of Fib-4, APRI or AST/ALT (Supplementary Table 4), indicating the aetiology-independence of the results obtained from analysis of the total population. Additionally, we did not find any association between sPDGFRβ levels and clinical features such as sex ($p = 0.2863$), age ($r = 0.1578$; $p = 0.0562$) (data not shown), and BMI ($r = 0.1132$; $p = 0.1863$) (Fig. 3b). Only a few parameters had significant correlation to sPDGFRβ, being ALT ($r = 0.1724$; $p = 0.0440$), alkaline phosphatase ($r = 0.1969$; $p = 0.0226$), total bilirubin ($r = 0.2990$; $p = 0.0005$), and albumin ($r = -0.1820$; $p = 0.0414$) (Fig. 3b). Their low correlation coefficient, and the fact that only a limited number of parameters correlate with sPDGFRβ, is explained by the hepatocyte-nature of most tested metabolic and biochemical parameters. This further underlines the HSC-origin of sPDGFRβ and its progressive increasing character in liver fibrosis.

3.6. Integration of sPDGFRβ into a novel diagnostic algorithm: the PRTA-score

To improve the diagnostic accuracy of sPDGFRβ, we generated an algorithm containing three factors that are all correlated with fibrosis progression (Fig. 3c): sPDGFRβ ($r = 0.3406$; $p < 0.0001$), albumin ($r = -0.2541$; $p = 0.00391$), and thrombocyte levels ($r = -0.3343$; $p < 0.0001$). When sPDGFRβ is combined with each individual factor, an increase in AUC can be seen for the prediction of significant fibrosis (sPDGFRβ/albumin: 0.7431; sPDGFRβ/thrombocytes: 0.7672), advanced fibrosis (sPDGFRβ/albumin: 0.6702; sPDGFRβ/thrombocytes: 0.7360), and cirrhosis (sPDGFRβ/albumin: 0.6938; sPDGFRβ/thrombocytes: 0.7701) (Table 3).

We combined these three factors into the sPDGFRβ thrombocyte albumin (PRTA)-score, using the following ratios:

$$\text{PRTA}-\text{score} = (\text{sPDGFR}\beta[\text{pg/mL}]^{*}\ 100)/(\text{albumin}[\text{g/L}]^{*}\ (\text{thrombocytes}[/\text{mm}^3]/100))$$

The PRTA-score can predict better significant fibrosis (0.7849 (95% CI: 0.6995–0.8702) and advanced fibrosis (0.7470 (95% CI 0.6586–0.8355), higher (Table 3) than Fib-4, APRI, and AST/ALT (Table 2). However, the predictive value for cirrhosis (0.7995 (95% CI: 0.7122–0.8868) remains lower that the AUC obtained by using the Fib-4 score: 0.8344 (95% CI: 0.7623–0.9605). The PRTA-score is independent of sex, as no significant differences ($p = 0.9185$) are observed between male (9.293[5.538;15.50]) and female (9.110[7.280;11.84]) patients. Additionally, no correlation has been found between BMI of the patients and outcome of the PRTA-score ($r = 0.1064$; $p = 0.2558$) (data not shown).

3.7. The PRTA-score is highly predictive for significant fibrosis independent of liver disease aetiology

We next compared the diagnostic accuracy of sPDGFRβ alone, with the PRTA-score, and with the most important, and most used, clinical score: Fib-4 scoring (Fig. 4). The prediction of significant fibrosis increased from 0.7303 (95% CI: 0.6395–0.8211) using sPDGFRβ alone (Table 2) to 0.7849 (95% CI: 0.6995–0.8702) using the PRTA-score (Table 3). With this cohort, this AUC is significantly higher than the AUC provided by the Fib-4 score: 0.6635 (95% CI: 0.5690–0.7581) (Table 2). Additionally, for prediction of significant fibrosis, using a cut-off value of 7.804, the PRTA-score had good sensitivity and specificity values, respectively 77.11% and 73.17% (Table 3). When the patient population is divided based on aetiology of liver disease, a comparable significant predictive function for significant liver fibrosis is seen (Supplementary Table 5) for viral liver disease: 0.7905 (95% CI: 0.6386–0.9423); NAFLD: 0.6809 (95% CI: 0.5249–0.8369); and alcoholic liver disease: 0.8641 (95% CI: 0.7301–1.025), which are all higher than the AUC values obtained by the clinical algorithms (Supplementary Table 4). Together these data suggest that the PRTA-score is superior to Fib-4, APRI, and AST/ALT for the diagnosis of significant liver fibrosis, independent of liver disease-aetiology.

3.8. Validation of the PRTA-score in an independent patient cohort

We next validated the PRTA-score in an independent patient cohort of 57 patients (Supplementary Table 6), with NAFLD, with histological assessment of fibrosis stage. Analysis of this cohort further validated the high predictive value of the PRTA-score (0.7284 (95% CI: 0.5868–0.8700)) as compared to those obtained by applying sPDGFRβ-levels `0.6702 (95% CI: 0.5192–0.8215) the Fib-4 score (0.6537 (95% CI: 0.4907–0.8168)) or NAFLD fibrosis score (0.6056 (95% CI: 0.4373–0.7737)) (Fig. 5a). Its important diagnostic value was further shown with its significant change ($p = 0.00059$) between patients with significant fibrosis (F ≥ 2) and those with no or mild fibrosis (F0–1) (Fig. 5b), The use of liver biopsy as reference method, allowed us to group patients with early stage liver fibrosis (F ≤ 2) into 2 populations: stage F1 and stage F2, to truly verify the accuracy of sPDGFRβ and the PRTA-score to distinguish between the early stages of liver fibrosis. While sPDGFRβ-levels were up-regulated in a non-significant manner, the PRTA-score was significantly ($p = 0.0386$) higher in the patient cohort with stage F2 liver fibrosis, compared to those with

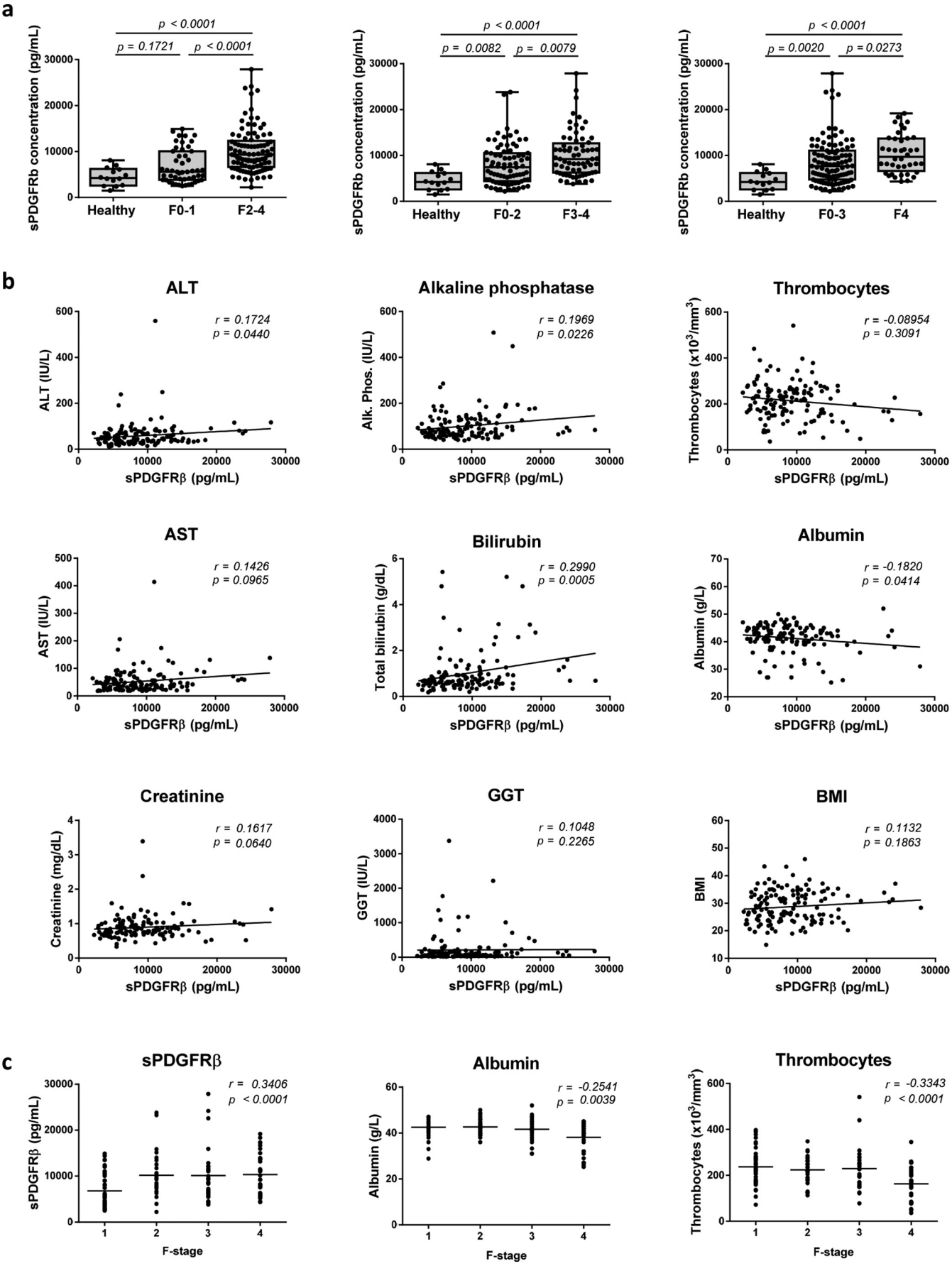
a
p < 0.0001
p = 0.1721
p < 0.0001
sPDGFRb concentration (pg/mL)
Healthy
F0-1
F2-4
p < 0.0001
p = 0.0082
p = 0.0079
Healthy
F0-2
F3-4
p < 0.0001
p = 0.0020
p = 0.0273
Healthy
F0-3
F4
b
ALT
r = 0.1724
p = 0.0440
ALT (IU/L)
sPDGFRβ (pg/mL)
Alkaline phosphatase
r = 0.1969
p = 0.0226
Alk. Phos. (IU/L)
Thrombocytes
r = -0.08954
p = 0.3091
Thrombocytes (x10³/mm³)
AST
r = 0.1426
p = 0.0965
AST (IU/L)
Bilirubin
r = 0.2990
p = 0.0005
Total bilirubin (g/dL)
Albumin
r = -0.1820
p = 0.0414
Albumin (g/L)
Creatinine
r = 0.1617
p = 0.0640
Creatinine (mg/dL)
GGT
r = 0.1048
p = 0.2265
GGT (IU/L)
BMI
r = 0.1132
p = 0.1863
BMI
c
sPDGFRβ
r = 0.3406
p < 0.0001
sPDGFRβ (pg/mL)
F-stage
Albumin
r = -0.2541
p = 0.0039
Albumin (g/L)
Thrombocytes
r = -0.3343
p < 0.0001
Thrombocytes (x10³/mm³)

Table 2
Accuracy of sPDGFRβ and the clinical scores Fib-4, APRI, and AST/ALT-ratio for the detection of significant fibrosis (F ≥ 2), advanced fibrosis (F ≥ 3), and cirrhosis (F = 4), in the total patient cohort.

	AUC	95% CI	*p*-value	Optimal Cut-off	Sensitivity (%)	Specificity (%)	PPV (%)	NPV (%)	Youden's index
sPDGFRβ (pg/mL)									
All patients									
F ≥ 2	0.7303	0.6395 to 0.8211	<0.0001	6003	82.47	62.00	80.49	65.03	0.4447
F ≥ 3	0.6446	0.5565 to 0.7327	0.002552	5861	82.35	40.51	54.06	72.97	0.2286
F = 4	0.6409	0.5457 to 0.7360	0.008703	7497	75.00	48.60	35.08	83.99	0.2360
Fib-4									
All patients									
F ≥ 2	0.6635	0.5690 to 0.7581	0.002295	1.495	65.52	68.18	79.66	50.97	0.3370
F ≥ 3	0.7123	0.6225 to 0.8022	< 0.0001	1.495	74.58	62.5	62.83	74.31	0.3708
F = 4	0.8344	0.7623 to 0.9065	<0.0001	1.495	93.94	59.18	46.01	96.34	0.5312
APRI									
All patients									
F ≥ 2	0.6309	0.5331 to 0.7286	0.01466	0.4849	44.83	79.55	80.66	43.12	0.2438
F ≥ 3	0.6723	0.5779 to 0.7667	0.0007139	0.5718	44.07	87.5	74.98	64.79	0.3157
F = 4	0.7965	0.7028 to 0.8902	<0.0001	0.7002	60.61	90.82	70.98	86.16	0.5143
AST/ALT ratio									
All patients									
F ≥ 2	0.5976	0.4952 to 0.7001	0.07019	1.174	28.41	90.7	85.32	39.98	0.1911
F ≥ 3	0.6423	0.5462 to 0.7383	0.005081	1.174	39.34	92.86	82.40	64.29	0.3220
F = 4	0.7486	0.6458 to 0.8515	<0.0001	1.184	55.88	91.75	71.49	84.88	0.4763

Fib-4: Fibrosis-4; AST/ALT-ratio: aspartate aminotransferase/alanine aminotransferase ratio; APRI: AST to platelet ratio index; AUC: Area under the curve; CI: Confidence interval; PPV: positive predictive value; NPV: negative predictive value.

Table 3
Accuracy of PRTA-score, sPDGFRβ/albumin, sPDGFRβ/thrombocyte numbers, and sPDGFRβ for the detection of significant fibrosis (F ≥ 2), advanced fibrosis (F ≥ 3), and cirrhosis (F = 4), in the total patient cohort.

	AUC	95% CI	p-value	Optimal Cut-off	Sensitivity (%)	Specificity (%)	PPV (%)	NPV (%)	Youden's index
PRTA-score									
All patients									
F ≥ 2	0.7849	0.6995 to 0.8702	<0.0001	7.804	77.11	73.17	84.54	62.69	0.5028
F ≥ 3	0.7470	0.6586 to 0.8355	<0.0001	9.979	70.91	78.26	73.49	75.99	0.4917
F = 4	0.7995	0.7122 to 0.8868	<0.0001	11.01	80.65	74.19	53.64	91.19	0.5484
[sPDGFRβ (pg/mL)/albumin (g/L)]									
All patients									
F ≥ 2	0.7431	0.6494 to 0.8369	<0.0001	140.0	85.88	54.76	78.31	67.09	0.4064
F ≥ 3	0.6702	0.5771 to 0.7633	0.001004	253.4	49.12	77.14	64.61	64.08	0.2626
F = 4	0.6938	0.5902 to 0.7973	0.001079	253.4	59.38	73.68	45.52	83.04	0.3306
[sPDGFRβ (pg/mL)/(thrombocytes (/mm^3)/100)]									
All patients									
F ≥ 2	0.7672	0.6808 to 0.8535	<0.0001	3.707	69.32	77.27	85.29	56.97	0.4659
F ≥ 3	0.7360	0.6487 to 0.8233	<0.0001	4.039	75.00	70.83	68.61	76.92	0.4583
F = 4	0.7701	0.6780 to 0.8622	<0.0001	4.589	76.47	74.49	52.61	89.52	0.5096
sPDGFRβ (pg/mL)									
All patients									
F ≥ 2	0.7303	0.6395 to 0.8211	<0.0001	6003	82.47	62.00	80.49	65.03	0.4447
F ≥ 3	0.6446	0.5565 to 0.7327	0.002552	5861	82.35	40.51	54.06	72.97	0.2286
F = 4	0.6409	0.5457 to 0.7360	0.008703	7497	75.00	48.60	35.08	83.99	0.2360

AUC: Area under the curve; CI: Confidence interval; PPV: positive predictive value; NPV: negative predictive value.

stage F1 liver fibrosis (Fig. 5c). Noteworthy, considering the high BMI values of these NAFLD-patients, we did not find any correlation between PRTA-levels and BMI-scores ($r = 0.1282$; $p = 0.3601$) (data not shown).

4. Discussion

Fibrosis progression is accompanied by increased PDGFRβ expression in activated HSCs [3]. We confirmed that PDGFRβ-expression is significantly dysregulated in human (Fig. 1d) and murine (Fig. 2a,b) subjects with liver fibrosis, and that HSCs are truly its most important source in the affected liver (Fig. 2c,d). We further investigated its diagnostic ability to detect significant fibrosis (F ≥ 2), advanced fibrosis (F ≥ 3), and cirrhosis (F = 4), in a patient population with different causes of liver disease. Circulating sPDGFRβ-levels were found to be highly elevated in patients with significant liver fibrosis (Fig. 3a), independently of the aetiology of the liver disease. We increased its diagnostic accuracy by combining it with albumin levels and thrombocyte

Fig. 3. sPDGFRβ expression in a cohort of patients ($n = 148$) with liver fibrosis due to chronic alcohol abuse, NAFLD or viral hepatitis. Patients with alcoholic or viral liver disease underwent FibroScan to determine the stage of liver fibrosis, while patients with NAFLD underwent ARFI. (a) Plasma sPDGFRβ levels in patients with increasing stage of fibrosis. (b) The relationship between plasma sPDGFRβ levels and biochemical and metabolic parameters. (c) Correlation of the three parameters of the PRTA-score, being sPDGFRβ, albumin and thrombocytes with fibrosis progression. Correlation parameters were calculated with Spearman's correlations test.

numbers into a novel diagnostic algorithm: the PRTA-score. Next, the diagnostic value of sPDGFRβ levels and the PRTA-score were confirmed in an independent NAFLD-patient cohort, with histological staging of fibrosis in liver biopsies (Fig. 5).

Serological markers are considered the ideal way for diagnosis, thanks to their non-invasive quality, easy implementation in routine analysis, low cost, dynamic character, and no inter-and intra-observer variability [28]. We previously identified an enhanced presence of PDGFRβ on EVs extracted from the circulation of patients with early fibrosis (F ≤ 2) caused by chronic HBV or HCV infection [18]. Concentrating solely on EVs as biomarkers for fibrosis would significantly weaken the clinical relevance as the current clinical setting is not yet ready for implementation of EV analysis in its work flow [8]. We therefore focused on total circulating sPDGFRβ, either EV-bound or freely circulating, and showed that the sPDGFRβ levels have a very good diagnostic value for significant liver fibrosis when integrated into the PRTA-score. Since albumin and thrombocyte levels are already integrated in the clinical setting as easy, cheap, and commercially available biochemical analysis panels, we expect only limited additional costs for integration of the PRTA-score. As our scoring system solely relies on the analysis of circulating factors, it can be executed in almost every clinical centre, which is in strong contrast to the exclusive presence of liver biopsy and transient elastography in large and well-equipped hospitals. Additionally, compared to these latter diagnostic manners, our PRTA-score only requires limited human resources, which reduces the eventual costs on the patient and health care system. We thus anticipate that this easy and cost-effective PRTA analysis could facilitate screening of at-risk patients, and thus identify those patients who need liver biopsy for more specific evaluation of the extent and potential cause of liver injury. Eventually, this could lead to an earlier therapeutic intervention, leading to a decline in liver-associated morbidity and mortality and a further reduction of the current financial weight on the health care system.

One of the major weaknesses of current clinical and experimental scoring systems for liver fibrosis, is their limited or non-existing validation in multiple aetiologies of liver disease. More precisely, most of the diagnostic studies focus on patients with chronic viral hepatitis, and thus can only speculate its utility in patients with other causes of liver disease [29]. We therefore put focus on the aetiology-independence of our newly developed PRTA-score, as demonstrated by its high AUC values for the diagnosis of significant liver fibrosis in each aetiology-specific patient cohort (Supplementary Tables 3 and 5) superior to those obtained by the clinical scores Fib-4, APRI, and AST/ALT ratio (Supplementary Table 4). Additionally, the cut-off values of the PRTA-score for diagnosis of significant liver fibrosis (Supplementary Table 5) are comparable between viral liver disease (7.748), NAFLD (7.321), and alcoholic liver disease (7.738), in contrast to the high variability between aetiologies observed in the other clinical scores (Supplementary Table 4). Such aetiology-independent cut-off values, and the possibility to use one consensus standard cut-off value would create uniformity in all clinical centres, which is currently not the case for some diagnostic tools for liver fibrosis e.g. transient elastography [20]. Finally, we validated the aetiology-independence of our PRTA-score in an independent patient cohort, consisting of NAFLD-patients with extremely high BMIs (44–57 kg/m^2). This cohort shows that potential negative effects of aetiology-specific characteristics, such as the high BMI and extensive liver steatosis did not affect the PRTA-score (Fig. 5).

This study does have some limitations. In particular, the number of included patients is relatively low. However, despite these low patient numbers, there is a good correlation of the results over all 3 aetiologies of liver disease which affirms the obtained results and encourages further study of the diagnostic utility of the PRTA-score. An inequality in patient numbers representing each stage of the fibrosis progression is also present (Supplementary Table 2). In the initial population, especially the stages significant ($n = 29$) and advanced ($n = 28$) fibrosis were less represented, as compared to mild fibrosis ($n = 51$) and cirrhosis ($n = 40$), what could have led to some inconsistent cut-off values.

As our validation patient cohort solely included biopsy-staged NAFLD-patients, future prospective studies should focus on the further validation of the obtained results in biopsy-staged patients with other aetiologies of liver disease. Effectuating elastography measurements and serological assessment on patients which underwent liver biopsy, requires a substantial investment, but could provide information on the possibility to replace costly imaging modalities by the PRTA score. Additionally, it would be interesting to include patients from longitudinal studies, in which the cause of injury was eliminated. The resolution of liver fibrosis is based on a decline of activated HSCs in the liver, prior to degradation of extracellular matrix (ECM) [30]. Current non-invasive diagnostic tools fail in the sensitive and specific follow-up of liver resolution, which is not that surprising, considering they often rely on ECM content evaluation, as applies to the ELF score and most of the imaging

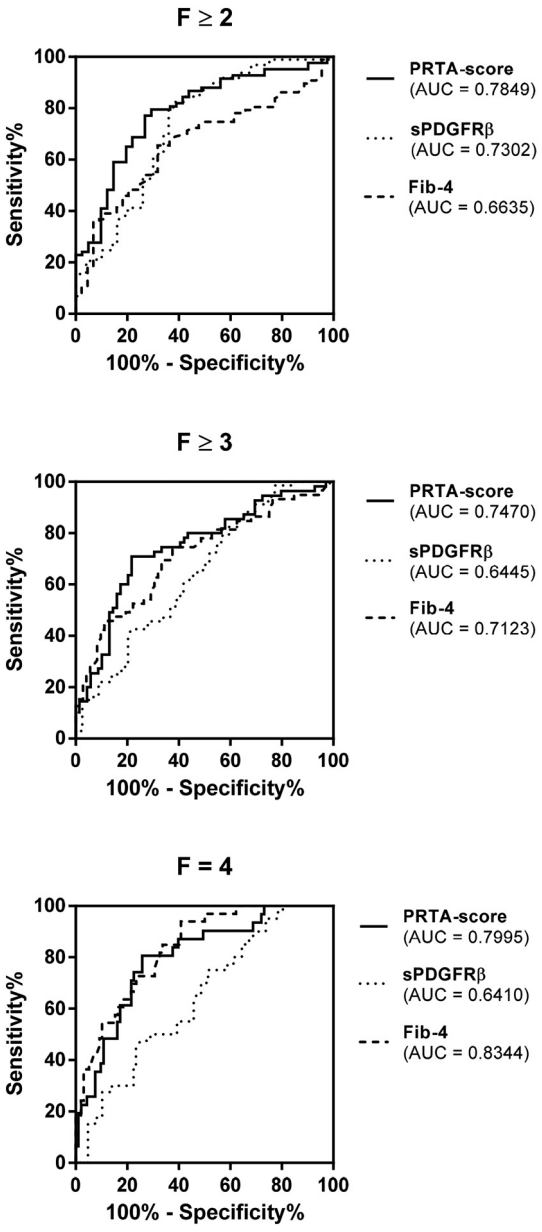

Fig. 4. Performance comparison of sPDGFRβ, PRTA-score and Fib-4 in the diagnosis of liver fibrosis/cirrhosis in a heterogeneous patient population. Receiver operating characteristic (ROC) curves for the non-invasive diagnosis of significant fibrosis (F ≥ 2), advanced fibrosis (F ≥ 3), and cirrhosis (F = 4) comparing sPDGFRβ levels, the sPDGFRβ-containing PRTA-score, and Fib-4 score.

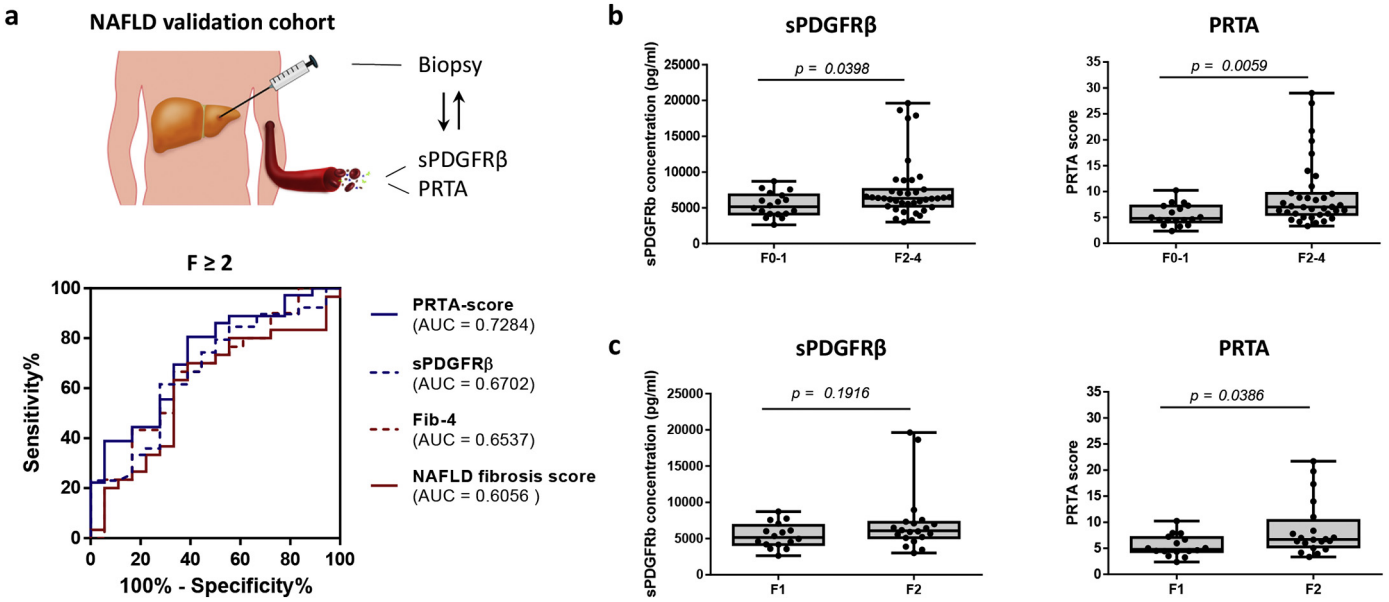

Fig. 5. Diagnostic performance of the PRTA-score in an independent validation patient cohort with NAFLD. sPDGFRβ-levels and the PRTA-score were determined on NAFLD-patients who underwent liver biopsy for precise staging of fibrosis. (a) Comparison of AUROC levels of sPDGFRβ, PRTA, Fib-4 and NAFLD fibrosis score for identification of significant fibrosis. (b) Separation of the patient cohort into patients with early (F0–1) and significant (F ≥ 2) fibrosis, for analysis of the PRTA-score or sPDGFRβ-levels alone. (c) Comparison of sPDGFRβ-levels and PRTA-score in patients staged with F = 1, to those staged with F = 2. Note that only the PRTA-score can significantly distinguish between patients with F1 and F2 fibrosis.

modalities. True early events of fibrosis resolution, being the deactivation and elimination of myofibroblasts due to senescence, apoptosis, and inactivation [30], are not considered by these scoring systems. We hypothesize that a reduction of activated HSCs, and thus PDGFRβ-positive cells, can be evaluated by circulating sPDGFRβ levels and the derived PRTA-score, providing better follow-up of fibrosis resolution. Follow up studies will aim at comparing the sensitivity to detect fibrosis resolution by the PRTA-score, liver biopsy and elastography. Additionally, the non-invasive character of the PRTA-score might also lead to a lower threshold to participate in clinical trials and their subsequent follow up studies, resulting in higher trial participation rates. As our research solely focused on the diagnostic value of circulating PDGFRβ, follow-up experiments investigating its mechanistical and functional role would be of great interest. In particular, functional differences between PDGFRβ sorted into EVs and those circulating as free proteins, could lead to novel insights in the intercellular communication mechanisms during liver fibrosis.

In conclusion, the current study demonstrates that the sPDGFRβ-containing PRTA-score is an accurate, inexpensive and simple scoring algorithm to diagnose significant liver fibrosis in a heterogeneous patient population. With validation in larger patient cohorts, this serological test could become an important tool for non-invasive clinical assessment of liver fibrosis in the future.

Acknowledgments

We would like to acknowledge Aneta Kozyra, Danielle Blyweert, and Iona De Mol for technical support. We thank Prof. Karin Vanderkerken for the use of the ZetaView® PMX110. We thank Dr. Bert Van den Bossche (Department of Hepatobiliary and Pancreas Surgery, ASZ Aalst) and prof. Daniel Jacobs-Tulleneers-Thevissen (Department of Thoracic and Transplantation Surgery and Surgical Oncology, University Hospital Brussels) for providing human tissue. We thank Prof. Niedergethmann and Dr. Hasenberg (Department for General- and Visceral Surgery, Alfried Krupp Hospital, Essen, Germany) for sample collection of the validation cohort. We also would like to thank Prof. Margarete Odenthal (Institute for Pathology, University Hospital Cologne), Prof. Hideo A. Baba (Institute for Pathology, University Hospital Essen), and Prof. Johannes Haybäck (Institute for Pathology, University Hospital Magdeburg) for histological preparation and assessments for the validation cohort.

Financial support

This work was supported by the Vrije Universiteit Brussel, the Institute for the Promotion of Innovation through Science and Technology in Flanders (IWT-Flanders) (HILIM-3D; SBO140045), and the Fund of Scientific Research Flanders (FWO) to LvG and IM. Funding sources had no involvement in the study design; in the collection, analysis, and interpretation of data; in the writing of the report; and in the decision to submit the paper for publication.

Conflicts of interest

JL and LvG are inventors of the pending patent “Soluble PDGFR beta as a biomarker for liver fibrosis”. No other potential conflicts of interest to disclose.

Author contributions

JL study concept and design; acquisition of data; analysis and interpretation of data; statistical analysis; drafting of the manuscript. SV analysis and interpretation of data. IM interpretation of data; critical revision of the manuscript. JPS, JB, and AC provision of samples; critical revision of the manuscript. HR provision of samples; interpretation of data; critical revision of the manuscript. LvG study concept and design; interpretation of data; critical revision of the manuscript.

Appendix A. Supplementary data

Supplementary data to this article can be found online at https://doi.org/10.1016/j.ebiom.2019.04.036.

References

[1] Bataller R, Brenner DA. Liver fibrosis. J Clin Invest 2005;115(2):209–18.

[2] Pinzani M, Marra F. Cytokine receptors and signaling in hepatic stellate cells. Semin Liver Dis 2001;21(3):397–416.
[3] Kocabayoglu P, Lade A, Lee YA, Dragomir AC, Sun X, Fiel MI, et al. beta-PDGF receptor expressed by hepatic stellate cells regulates fibrosis in murine liver injury, but not carcinogenesis. J Hepatol 2015;63(1):141–7.
[4] Pinzani M. PDGF and signal transduction in hepatic stellate cells. Front Biosci 2002; 7:d1720-6.
[5] Regev A, Berho M, Jeffers LJ, Milikowski C, Molina EG, Pyrsopoulos NT, et al. Sampling error and intraobserver variation in liver biopsy in patients with chronic HCV infection. Am J Gastroenterol 2002;97(10):2614–8.
[6] Cadranel JF, Rufat P, Degos F. Practices of liver biopsy in France: results of a prospective nationwide survey. For the group of epidemiology of the French association for the study of the liver (AFEF). Hepatology 2000;32(3):477–81.
[7] Pasha T, Gabriel S, Therneau T, Dickson ER, Lindor KD. Cost-effectiveness of ultrasound-guided liver biopsy. Hepatology 1998;27(5):1220–6.
[8] Lambrecht J, Verhulst S, Mannaerts I, Reynaert H, van Grunsven LA. Prospects in non-invasive assessment of liver fibrosis: liquid biopsy as the future gold standard? Biochim Biophys Acta Mol Basis Dis 2018;1864(4 Pt A):1024–36.
[9] Kennedy P, Wagner M, Castera L, Hong CW, Johnson CL, Sirlin CB, et al. Quantitative elastography methods in liver disease: current evidence and future directions. Radiology 2018;286(3):738–63.
[10] Sandrin L, Fourquet B, Hasquenoph JM, Yon S, Fournier C, Mal F, et al. Transient elastography: a new noninvasive method for assessment of hepatic fibrosis. Ultrasound Med Biol 2003;29(12):1705–13.
[11] Friedrich-Rust M, Nierhoff J, Lupsor M, Sporea I, Fierbinteanu-Braticevici C, Strobel D, et al. Performance of acoustic radiation force impulse imaging for the staging of liver fibrosis: a pooled meta-analysis. J Viral Hepat 2012;19(2):e212-9.
[12] Sterling RK, Lissen E, Clumeck N, Sola R, Correa MC, Montaner J, et al. Development of a simple noninvasive index to predict significant fibrosis in patients with HIV/HCV coinfection. Hepatology 2006;43(6):1317–25.
[13] Rosenberg WM, Voelker M, Thiel R, Becka M, Burt A, Schuppan D, et al. Serum markers detect the presence of liver fibrosis: a cohort study. Gastroenterology 2004;127(6):1704–13.
[14] Williams AL, Hoofnagle JH. Ratio of serum aspartate to alanine aminotransferase in chronic hepatitis. Relationship to cirrhosis. Gastroenterology 1988;95(3):734–9.
[15] Wai CT, Greenson JK, Fontana RJ, Kalbfleisch JD, Marrero JA, Conjeevaram HS, et al. A simple noninvasive index can predict both significant fibrosis and cirrhosis in patients with chronic hepatitis C. Hepatology 2003;38(2):518–26.
[16] European Association for Study of L, Asociacion Latinoamericana para el Estudio del H. EASL-ALEH clinical practice guidelines: non-invasive tests for evaluation of liver disease severity and prognosis. J Hepatol 2015;63(1):237–64.
[17] Dulai PS, Singh S, Patel J, Soni M, Prokop LJ, Younossi Z, et al. Increased risk of mortality by fibrosis stage in nonalcoholic fatty liver disease: systematic review and meta-analysis. Hepatology 2017;65(5):1557–65.
[18] Lambrecht J, Jan Poortmans P, Verhulst S, Reynaert H, Mannaerts I, van Grunsven LA. Circulating ECV-associated miRNAs as potential clinical biomarkers in early stage HBV and HCV induced liver fibrosis. Front Pharmacol 2017;8:56.
[19] Stradiot L, Verhulst S, Roosens T, Oie CI, Moya IM, Halder G, et al. Functionality based method for simultaneous isolation of rodent hepatic sinusoidal cells. Biomaterials 2017;139:91–101.
[20] Friedrich-Rust M, Ong MF, Martens S, Sarrazin C, Bojunga J, Zeuzem S, et al. Performance of transient elastography for the staging of liver fibrosis: a meta-analysis. Gastroenterology 2008;134(4):960–74.
[21] Kleiner DE, Brunt EM, Van Natta M, Behling C, Contos MJ, Cummings OW, et al. Design and validation of a histological scoring system for nonalcoholic fatty liver disease. Hepatology 2005;41(6):1313–21.
[22] Desmet VJ, Gerber M, Hoofnagle JH, Manns M, Scheuer PJ. Classification of chronic hepatitis: diagnosis, grading and staging. Hepatology 1994;19(6):1513–20.
[23] Youden WJ. Index for rating diagnostic tests. Cancer 1950;3(1):32–5.
[24] Raposo G, Stoorvogel W. Extracellular vesicles: exosomes, microvesicles, and friends. J Cell Biol 2013;200(4):373–783.
[25] Pinzani M, Milani S, Herbst H, DeFranco R, Grappone C, Gentilini A, et al. Expression of platelet-derived growth factor and its receptors in normal human liver and during active hepatic fibrogenesis. Am J Pathol 1996;148(3):785–800.
[26] Cao S, Yaqoob U, Das A, Shergill U, Jagavelu K, Huebert RC, et al. Neuropilin-1 promotes cirrhosis of the rodent and human liver by enhancing PDGF/TGF-beta signaling in hepatic stellate cells. J Clin Invest 2010;120(7):2379–94.
[27] Starkel P, Leclercq IA. Animal models for the study of hepatic fibrosis. Best Pract Res Clin Gastroenterol 2011;25(2):319–33.
[28] Baranova A, Lal P, Birerdinc A, Younossi ZM. Non-invasive markers for hepatic fibrosis. BMC Gastroenterol 2011;11:91.
[29] Motola DL, Caravan P, Chung RT, Fuchs BC. Noninvasive biomarkers of liver fibrosis: clinical applications and future directions. Curr Pathobiol Rep 2014;2(4):245–56.
[30] Tacke F, Trautwein C. Mechanisms of liver fibrosis resolution. J Hepatol 2015;63(4): 1038–9.